

– R), and $D = (k_{E3} + R)(k_{E4} + R)$. Solving the $\dot{X} = 0$ equation for Y yields

$$Y = (EX - 2k_{L1}X^2 + Ak_{L2})/k_{E2}X \quad (3)$$

where $E = k_{E1}A\alpha - R$. The intersections of eq 2 and 3 in the X - Y plane are the steady states of the system. A schematic plot of eq 2 and 3 is shown in Figure 1. There is only one intersection in the positive quadrant, and it is apparent that this fact is independent of the rate constant values chosen. It is a result of the basic form of the Explodator. Figure 1 was constructed assuming that $k_{E3}\beta > R$ and that $k_{E1}\alpha A > R$, physically reasonable assumptions.⁶ However, the result that there is only one intersection in the positive quadrant does not change if these conditions are violated.

An additional limiting reaction, L5, is suggested by the form



of the Oregonator. It corresponds in that model to the production of HBrO_2 by the reaction of bromate and bromide ions. Replacement of reaction L2 by reaction L5 does not change eq 2 except that D is now defined by $D = (k_{E3} + R)(k_{E4} + R + k_{L5})$. Equation 3 becomes

$$Y = (EX - 2k_{L1}X^2)/(k_{E2}X - k_{L5}) \quad (4)$$

Figure 2 shows schematic plots of eq 2 and 4. It is again apparent

that there can be only one positive steady state, regardless of the values chosen for the rate parameters.

The same methods show clearly bistability in the Oregonator. Figure 3 show schematic plots of eq 5 and 6. The three steady

$$Y = ((fk_3k_5A)X/(k_5 + R) + RY_0)/(k_1A + k_2X + R) \quad (5)$$

$$Y = ((k_3A - R)X - k_4X^2)/(k_2X - k_1A) \quad (6)$$

states are apparent as three intersections in the positive quadrant. The numbering in eq 5 and 6 is after Field and Noyes.⁹ The behavior of the Oregonator is more sensitive to rate constant values than is the Explodator. The three intersections in the positive quadrant only appear for certain parameter values. For the parameters used by DeKepper and Boissonade⁶ in their study of bistability in the BZ reaction, the steady-state values calculated from eq 4 and 5 are $X = 3.1575 \times 10^{-12}$ M, 4.842×10^{-9} M, and 2.550×10^{-7} M.

We conclude that the Explodator cannot model bistability, a most important characteristic of oscillating chemical reactions. It is thus only a suitable model for a chemical oscillator which does not exhibit bistability. We know of no such halogen-based chemical oscillator. It may well be that a chemical oscillator will eventually be found whose dynamics are related to the Explodator, but none seems to be known presently.

Acknowledgment. This work was partially supported by the National Science Foundation under Grant CHE80-23755.

Temperature Effects on Rates of Dehalogenation of Aromatic Anion Radicals

M. Meot-Ner (Mautner),* P. Neta,

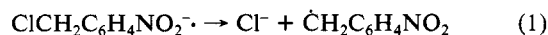
Chemical Kinetics Division, Center for Chemical Physics, National Bureau of Standards, Gaithersburg, Maryland 20899

Robert K. Norris, and Karen Wilson

Department of Organic Chemistry, The University of Sydney, N.S.W. 2006, Australia
(Received: May 29, 1985)

The temperature dependence of the unimolecular dehalogenation of radical anions of nitrobenzyl halides and haloacetophenones was measured between -7 and 70 °C. Activation parameters range from $E_a = 11.2$ – 16.9 kcal/mol and $\log A = 12.7$ – 17.1 . Both E_a and $\log A$ increase from *p*- to *o*-nitro radicals and from chloro to bromo radicals. Unfavorable steric effects that move the halogen atom out of the aromatic plane result in lowered A factors. In general, the variation of k_{294} with structure depends in a complex way on the combination of E_a and $\log A$ factors, which suggests caution in the evaluation of rate constants at one temperature. The fast unimolecular dissociation of $(p\text{-NO}_2\text{C}_6\text{H}_4\text{CH}_2\text{Br})^{\cdot-}$ ($k_{294} = 4.6 \times 10^5 \text{ s}^{-1}$) allows measurement of the slower bimolecular electron transfer $(\text{C}_6\text{H}_5\text{NO}_2)^{\cdot-} + p\text{-NO}_2\text{C}_6\text{H}_4\text{CH}_2\text{Br} \rightarrow (p\text{-NO}_2\text{C}_6\text{H}_4\text{CH}_2\text{Br})^{\cdot-} + \text{C}_6\text{H}_5\text{NO}_2$ ($k_{294} = 1.9 \times 10^6 \text{ M}^{-1} \text{ s}^{-1}$). Both the activation energy and probability factor contribute to the slow rate, possibly due to a geometry change upon the reduction of ArNO_2 . Extending the temperature studies to supercooled solutions shows no discontinuity of the unimolecular rate constants near the phase transition temperatures.

Halogen-substituted aromatic anion radicals are known to undergo dehalogenation to form a halide ion and a carbon-centered radical.¹ The dissociation shown in reaction 1, for example, is



important in the $\text{S}_{\text{RN}}1$ reaction of nitrobenzyl halides. The rate constants of dehalogenation were measured almost exclusively at room temperature and found to vary over many orders of mag-

nitude (basically limited on the one hand by the formation rate of the anion radical and on the other hand by the lifetime of the anion radical with respect to second-order decay). The effects of the nature of the halogen and of the other substituent as well as their relative positions in the molecule on the rate of dehalogenation have been discussed.²⁻⁷ Such comparisons, when based

(2) Neta, P.; Behar, D. *J. Am. Chem. Soc.* **1980**, *102*, 4798.

(3) Behar, D.; Neta, P. *J. Phys. Chem.* **1981**, *85*, 690.

(4) Neta, P.; Behar, D. *J. Am. Chem. Soc.* **1981**, *103*, 103.

(5) Behar, D.; Neta, P. *J. Am. Chem. Soc.* **1981**, *103*, 2280.

(6) Bays, J. P.; Blumer, S. T.; Baral-Tosh, S.; Behar, D.; Neta, P. *J. Am. Chem. Soc.* **1983**, *105*, 320.

(7) Norris, R. K.; Barker, S. D.; Neta, P. *J. Am. Chem. Soc.* **1984**, *106*, 3140.

(1) For review see: (a) Kornblum, N. In "The Chemistry of Functional Groups. Supplement F"; Patai, S., Ed.; Wiley: Chichester, U.K., 1982; Part 1, Chapter 10. (b) Norris, R. K. In "The Chemistry of Functional Groups. Supplement D"; Patai, S., Rappoport, Z., Eds.; Wiley: Chichester, U.K., 1983; Part 1, Chapter 16.

only on rate measurements at ambient temperatures, may lead to fortuitous conclusions depending on whether enthalpy and entropy effects support or oppose each other. Therefore, it is desirable to measure the temperature effects on these reactions. Representative examples are reported here.

Experimental Section

We have chosen representative compounds of those examined in the previous studies and prepared several new derivatives as well. The materials used and the experimental procedures are similar to those described previously. All solutions contained 10% alcohol in water and 2×10^{-4} to 1×10^{-3} M of the aromatic compound, either at pH 7 with 1×10^{-3} M phosphate buffer or at pH 11–12. The choice of pH and alcohol (*t*-BuOH or *i*-PrOH) was based upon the arguments detailed in the previous papers.^{2–7} The solutions were deoxygenated by bubbling with ultrahigh purity nitrogen. The bulk solutions were kept at room temperature throughout the experiment and were passed through a loop of quartz tubing immersed in a thermostated fluid and then through the irradiation cell which was also in contact with the thermostated fluid on three sides. The temperature was measured (to ± 0.5 °C) by a thermocouple immersed in the solution at the point of exit from the cell. Pulse irradiation was carried out with 50-ns electron pulses from a 2-MeV Febetron supplying about 500 rd/pulse. The kinetic spectrophotometric detection system and signal processing were as described before.⁸ The reactions of the primary radicals of water radiolysis leading to the formation of the aromatic anion radicals, as well as the spectral parameters of the intermediates and the wavelengths used for kinetic observations in each case, were given in detail before.^{2–7} Most kinetic measurements were carried out at one wavelength. The temperature was varied between -7 and 85 °C in small steps as shown in the figures. The rate constant at each temperature was measured 2–4 times. The average standard deviation of replicate measurements was 0.04 log k units, and the points shown in Figures 1 and 2 are average values from replicate measurements.

Syntheses. The general experimental procedures are as previously stated,⁷ with the additional note that preparative GLC was performed on a Hewlett Packard 776 at 140 °C with a 20% W98 column and preparative HPLC was performed on a Waters 510 system with a Whatman column (Partsil 10 M 20) with 0.8% ethyl acetate/light petroleum at a flow rate of 13 mL/min. With the exception of the four compounds below, all the compounds in this study have been prepared previously.^{6,7}

Nitro- α -bromo-*o*-xylenes. *o*-Xylene was nitrated by the literature procedure⁹ and the two mononitro derivatives were separated by preparative GLC. 4-Nitro-*o*-xylene was brominated by the literature procedure¹⁰ and the crude product was fractionated by flash chromatography on silica gel to give a mixture of the two monobromo compounds. Separation of this mixture by preparative HPLC gave the following:

2-Methyl-4-nitrobenzyl bromide: mp 52 – 53 °C (light petroleum); $^1\text{H NMR}$ δ 2.51 (s, 3 H, Me), 4.51 (s, 2 H, CH_2), 7.48 (d, 1 H, H₆, $J = 8.4$ Hz), 8.02 (dd, 1 H, H₅, $J = 8.4$ and 2.5 Hz), 8.06 (d, 1 H, H₃, $J = 2.5$ Hz); IR (CHCl_3) 1520, 1350 cm^{-1} ; UV (EtOH) 276 nm ($\epsilon 1.02 \times 10^4$); mass spectrum, m/z 231 ($\text{M}^+ + 2$, 10%), 229 (M^+ , 10), 150 (100), 120 (5), 110 (3), 103 (13), 92 (18), 78 (12), 63 (6), 51 (10).

Anal. Calcd for $\text{C}_8\text{H}_8\text{NO}_2\text{Br}$: C, 41.76; H, 3.51; N, 6.09. Found: C, 41.64; H, 3.64; N, 6.33.

2-Methyl-5-nitrobenzyl bromide: mp 77 – 79 °C (CH_2Cl_2 /light petroleum); $^1\text{H NMR}$ δ 2.51 (s, 3 H, Me), 4.53 (s, 2 H, CH_2), 7.35 (d, 1 H, H₃, $J = 8.3$ Hz), 8.06 (dd, 1 H, H₄, $J = 8.3$ and 2.4 Hz), 8.18 (d, 1 H, H₆, $J = 2.4$ Hz); IR (CHCl_3) 1518, 1345 cm^{-1} ; UV (EtOH) 218 nm ($\epsilon 1.42 \times 10^5$), 274 (8.5×10^4); mass

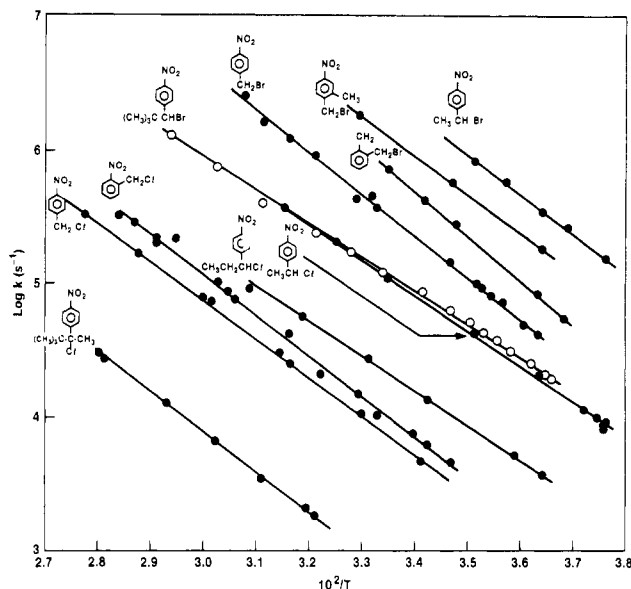


Figure 1. Arrhenius plots for the unimolecular dehalogenation of radical anions.

spectrum, m/z 231 ($\text{M}^+ + 2$, 4%), 229 (M^+ , 4), 150 (100), 104 (15), 92 (12), 78 (12), 63 (6), 51 (8).

Anal. Calcd for $\text{C}_8\text{H}_8\text{NO}_2\text{Br}$: C, 41.76; H, 3.51; N, 6.09. Found: C, 41.98; H, 3.53; N, 5.83.

In similar fashion treatment of 3-nitro-*o*-xylene gave the following:

2-Methyl-6-nitrobenzyl bromide: mp 61 – 62 °C (CH_2Cl_2 /light petroleum); $^1\text{H NMR}$ δ 2.52 (s, 3 H, Me), 4.71 (s, 2 H, CH_2), 7.32 (dd, 1 H, H₄, $J = 7.5$ and 7.8 Hz), 7.45 (dd, 1 H, H₃, $J = 7.8$ and 2.0 Hz), 7.72 (dd, 1 H, H₅, $J = 7.5$ and 2.0 Hz); IR (CHCl_3) 1525, 1350 cm^{-1} ; UV (EtOH) 221 nm ($\epsilon 1.25 \times 10^4$), 258 infl. (3.6×10^4); mass spectrum, m/z 231 ($\text{M}^+ + 2$, 4%), 229 (M^+ , 4), 183 (2), 150 (88), 133 (17), 122 (23), 119 (25), 107 (14), 106 (74), 104 (55), 103 (65), 102 (25), 92 (85), 91 (100), 79 (59), 78 (66), 77 (79), 65 (56).

Anal. Calcd for $\text{C}_8\text{H}_8\text{NO}_2\text{Br}$: C, 41.76; H, 3.51; N, 6.09. Found: C, 41.73; H, 3.54; N, 6.08.

2-Methyl-3-nitrobenzyl bromide: mp $155/0.7$ mmHg (Kugelrohr); $^1\text{H NMR}$ 2.51 (s, 3 H, Me), 4.54 (s, 2 H, CH_2), 7.28 (dd, 1 H, H₅, $J = 7.6$ and 7.9 Hz), 7.55 (dd, 1 H, H₆, $J = 7.6$ and 1.5 Hz), 7.71 (dd, 1 H, H₄, $J = 7.9$ and 1.5 Hz); IR (CHCl_3) 1525, 1350 cm^{-1} ; UV (EtOH) 223 nm ($\epsilon 1.52 \times 10^4$); mass spectrum, m/z 231 ($\text{M}^+ + 2$, 9%), 229 (M^+ , 9), 214 (8), 212 (8), 150 (100), 132 (14), 104 (36), 103 (87), 92 (28), 91 (26), 78 (38), 77 (54), 63 (17).

Anal. Calcd for $\text{C}_8\text{H}_8\text{NO}_2\text{Br}$: C, 41.76; H, 3.51; N, 6.09. Found: C, 41.92; H, 3.77; N, 6.38.

Certain commercial equipment, instruments, or materials are identified in this paper in order to specify adequately the experimental procedure. Such identification does not imply recognition or endorsement by the National Bureau of Standards, nor does it imply that the material or equipment identified are necessarily the best available for the purpose.

Results and Discussion

Arrhenius plots for the dehalogenation reactions of a variety of anion radicals are shown in Figures 1 and 2. The rate constants, activation energies, and A factors derived from these measurements are summarized in Table I. The standard deviation of the slopes and intercepts of the plots yield average error estimates of ± 0.2 for log A and ± 0.2 kcal/mol for E_a .

The measured rate constants in Table I span the range 6×10^2 to about 6×10^6 s^{-1} . The range is defined by experimental constraints. On the slow side, second-order decay of the radicals may become competitive for $k \sim 10^3$ s^{-1} , since under our experimental conditions the concentration of radicals produced by the pulse is $\sim 3 \times 10^{-6}$ M and the second-order decay of the anion radicals may be very rapid ($k \sim 10^8$ – 10^9 M^{-1} s^{-1} for aceto-

(8) Simic, M. G.; Hunter, E. P. L. In "Radioprotectors and Anticarcinogens"; Nygaard, O. F., Simic, M. G., Eds.; Academic Press: New York, 1983; p 449.

(9) Crossley, A. W.; Renouf, N. *J. Chem. Soc.* 1909, 95, 202.

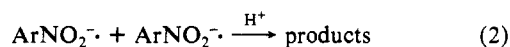
(10) Swee Hock Goh; Hooi Long Gian, *J. Chem. Soc., Perkin Trans. 1* 1979, 1625.

TABLE I: Activation Parameters for Rates of Dehalogenation of Anion Radicals

no.	compd	E_a , kcal/mol	log A	calcd k_{294} , s^{-1}	reported ^a $k_{room\ temp}$
1		13.3	13.7	7.6×10^3	4×10^3
2	(in neat H ₂ O)	13.4	13.6	5.0×10^3	
3	(in neat <i>i</i> -PrOH)	14.0	14.9	3.6×10^4	
4		13.8	14.1	8.1×10^3	1.0×10^4
5		12.3	14.0	8.3×10^4	9.7×10^4
6		12.0	13.0	1.4×10^4	
7		13.7	12.8	4.8×10^2	4×10^2
8		14.0	16.0	4.6×10^5	1.7×10^5
9		13.2	15.7	8.9×10^5	
10		15.5	17.1	4.5×10^5	4.0×10^5
11		13.8	16.8	4.1×10^6	3.5×10^6
12		11.2	13.3	1.1×10^5	6.2×10^4
13		12.3	12.7	4.1×10^3	1.5×10^3
14		14.5	16.4	4.9×10^5	5×10^5
15		16.9	16.0	3.3×10^3	5×10^3
16		16.1	17.1	1.6×10^5	1.4×10^5
17		14.9	13.7	4.9×10^2	4×10^2
18		12.7	13.9	3.3×10^4	4.2×10^4
19		Bimolecular Reactions 4.6			
20		6.0	10.7	1.9×10^6 ^b	

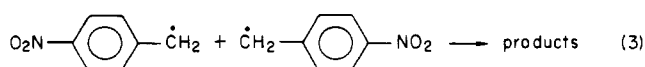
^a References 2-7. ^b In $M^{-1} s^{-1}$.

phenones¹¹ but considerably less for nitrobenzenes,¹² with reaction 2 being pH dependent). Examples for the contribution of sec-



ond-order decay are shown in the Arrhenius plots for *o*-chloroacetophenone and *p*-bromobenzaldehyde anions, where apparent deviations occur at low temperatures (and slow reactions) due to

this effect. As a result of this effect, the rate constants measured for these compounds at room temperature in fact contain a considerable contribution from second-order decay (which is impossible to discern without studying the temperature effect). Fortunately, the activation energies of the second-order reactions are only of the order of 4-6 kcal/mol. In the present systems, this was verified by measuring the activation energy for reaction 3 where $E_a = 4.6$ kcal/mol was found. Since the activation



energies of the unimolecular reactions are higher, 11-17 kcal/mol,

(11) Hayon, E.; Iyata, T.; Lichtin, N. N.; Simic, M. *J. Phys. Chem.* **1972**, *76*, 2072.

(12) Asmus, K. D.; Wigger, A.; Henglein, A. *Ber. Bunsenges. Phys. Chem.* **1966**, *70*, 862.

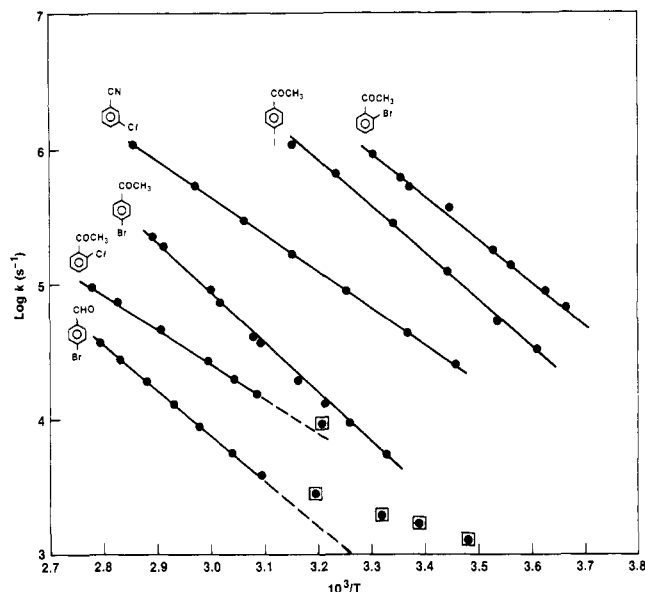


Figure 2. Arrhenius plots for the unimolecular dehalogenation of radical anions. Points in squares deviate from Arrhenius due to second-order reactions (see text).

the rates of the unimolecular reactions increase with temperature faster than the bimolecular reactions. Therefore, the unimolecular processes become significantly faster than bimolecular decay at high temperatures for the above systems, and thus the bimolecular processes do not interfere with the measurements of the unimolecular reactions at high temperatures. We also note that second-order contributions do not seem to occur in nitro compounds, where, as we noted, the second-order rate constants for reaction 2 are low.

On the fast side, unimolecular reactions must be substantially slower than the formation processes such as reaction 4. The rate



of (4) is limited by the rate constant (usually of the order of $10^{10} M^{-1} s^{-1}$)¹³ and the concentration of $ArNO_2$, which may be limited in water.

The accessible values for reactions actually measured at 294 K fall within the limits defined by the measurable rate constants $3.2 < \log k_{294} < 6.4$, and the corresponding lines, $\log A = 3.2 + E_a/2.3(294R)$ and $\log A = 6.4 + E_a/2.3(294R)$. (By working at lower or higher temperatures, these limits can be somewhat extended, i.e., rate constants that are too fast or too slow at 294 K can be measured.) Significantly, these limits impose an artificial, if broad, correlation between $\log A$ and E_a . As a result, combinations of extremely low $\log A$ and high E_a values, or vice versa, cannot appear in our data. Indeed, a coarse correlation of $\log A$ and E_a is noted (Figure 3). Since compensating enthalpy-entropy relations are frequent, it is important to realize that this may result in part, as in the present case, by observational selectivity.

Within the accessible range, both $\log A$ and E_a vary widely, i.e., 12–17 units and 11–17 kcal/mol, respectively (Table I). The limited number of examples in the table cover a variety of nitrobenzyl halides and haloacetophenones, as well as chlorobenzonitrile and bromobenzaldehyde. It is difficult, therefore, to establish the detailed effects of structure and substituents on the energetics of the dehalogenation reactions. Nevertheless, several trends emerge.

The preexponential factor appears to increase with the size of the halogen (Cl < Br < I) indicating the greater steric probability of electron transfer to the larger halogen. The activation energy, on the other hand, is greater for bromo than for chloro derivatives (experiments 8, 1; 10, 4; 11, 5 in Table I) but appears to decrease

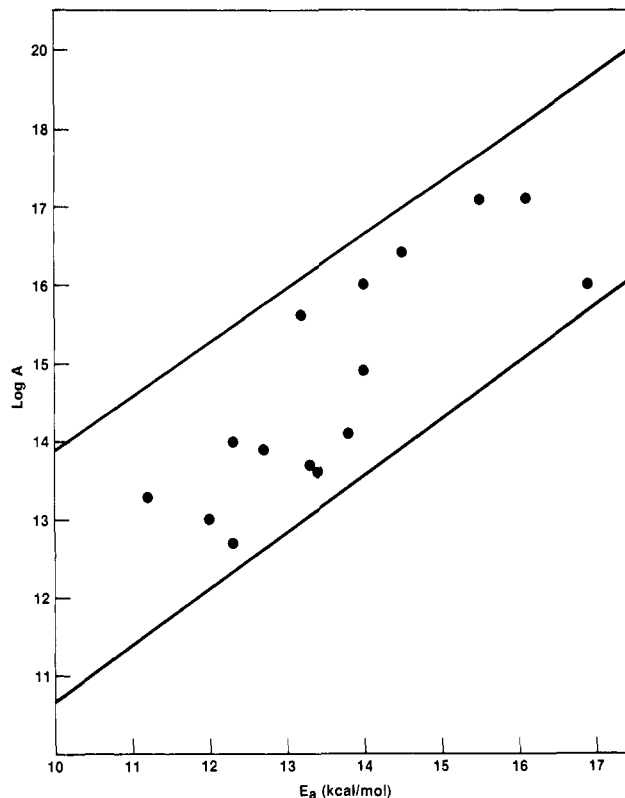


Figure 3. Correlation between E_a and $\log A$. Lines show limits defined by the slowest rate constant ($\log k_{294} = 3.2$) and the fastest rate constant ($\log k_{294} = 6.4$).

for iodo (15, 16). This may reflect opposing effects on the activation energy, i.e., carbon-halogen bond strength (Cl > Br > I) and electron affinity of the halogen.

The sterically hindered *tert*-butyl substituted nitrobenzyl halides (7, 12) exhibit lower A values than the corresponding nonhindered compounds (5, 8), indicating that the decreased rates of dehalogenation in these anion radicals are indeed owing to steric effects.⁷ On the other hand, while the activation energy for the chloro derivatives (5, 7) increases upon substitution with the *tert*-butyl group, it decreases considerably in the case of the bromo derivatives (8, 12). The latter decrease is somewhat unexpected, unless one assumes that the bulkiness of both *t*-Bu and Br (in 12) causes a decrease in the C-Br bond energy.

It is interesting to note also the trends in A upon α -substitution with methyl and ethyl. Methyl substitution increases A (1, 5 and 8, 11) while ethyl decreases A (1, 6) and *tert*-butyl decreases it further. This comparison may suggest that methyl substitution increases the probability of the halogen being in a conformation favorable for electron transfer (i.e., C-X in a plane perpendicular to the ring) while larger groups start twisting it away from this conformation. Methyl substitution at α -carbon also lowers the activation energy by decreasing the C-X bond dissociation energy.

The effect of a methyl group ortho to a CH_2Br group on the rate of dehalogenation of *p*-nitrobenzyl bromide demonstrates the importance of examining the temperature dependence of the rate constants. While the presence of the additional methyl group increases the rate of dehalogenation, this increase results from the operation of different factors, i.e., the reduction in E_a has greater effect than the decrease in $\log A$. In the meta system, where $k_1 = 60 s^{-1}$ was reported² for 3-O₂NC₆H₄CH₂Br, methyl substitution at position 2 or 4 was found to decrease the rate constant, but because of the low rates and the contributions of second-order reactions it was not possible to measure the activation parameters for these processes.

Comparing *o*- vs. *p*-nitrobenzyl chloride and bromide (1, 4 and 8, 10) both E_a and A are found to increase in the ortho derivative. These compensating effects result in little change in the rate constant at room temperature. The increase in A , however, clearly demonstrates the contribution of "through space" electron transfer

(13) Anbar, M.; Bambenek, M.; Ross, A. B. *Natl. Stand. Ref. Data Ser. (U.S., Natl. Bur. Stand.)* 1973, Report No. 43.

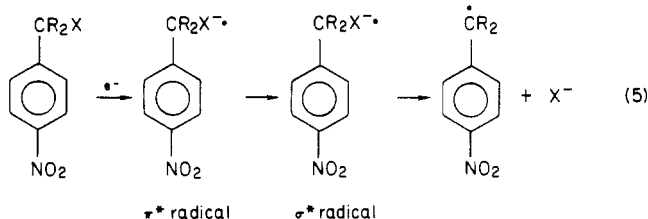
in the ortho derivatives, as discussed before.² The increase in E_a can be related to the lower spin density at the ortho vs. the para position.²

Other changes in E_a and A are seen in Table I when the substituents (NO_2 , COCH_3 , CHO , CN) are varied. It is difficult to draw conclusions from the limited number of examples given here. They demonstrate, however, that simple comparison of kinetics at room temperature does not permit full understanding of structural effects on dehalogenation rates of radical anions.

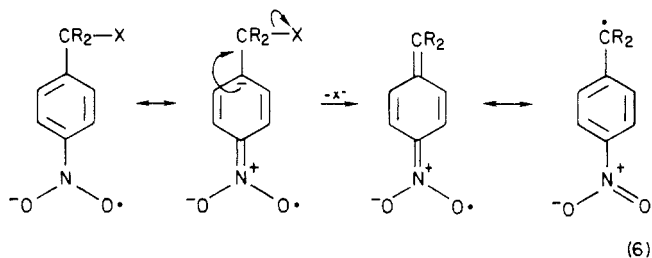
We also note an interesting solvent effect. While the activation parameters for dehalogenation rates in water and in 10% *i*-PrOH are equal, both E_a and A increase in neat *i*-PrOH. The increase in E_a may be due to decreased efficiency in the solvation of the product Cl^- ion.¹⁴ The reason for the increase in A is not clear. Here again the E_a and A vary in a compensating manner, leading to a change in k_{294} by a factor of 7.

It is interesting to compare the present results with the published temperature effects on rates of intramolecular electron-transfer reactions, which were studied only in several cases. Very low activation energies (~ 3 kcal/mol) were found for the cases of ruthenium-modified cytochrome *c*¹⁵ and 6-[*N*-(4-methylphenyl)amino]-2-naphthalenesulfonic acid *N,N*-dimethylamide¹⁶ and in both cases the rate-limiting step was suggested to be other than the electron transfer. Higher values were found for the intramolecular electron transfer from tyrosine to oxidized tryptophan radical in β -lactoglobulin (11 kcal/mol)¹⁷ and from Ru(II) to Co(III) bound through a short chain of isonicotinoyl and several amino acid residues (10–20 kcal/mol).¹⁸ These values are in the same range as the activation energies determined for the dehalogenation reactions in Table I. This similarity, however, need not imply similar mechanisms.

The dissociation of the radical anions of *p*-nitrobenzylic halides has been viewed as an intramolecular electron-transfer process, whereby an electron, added to the π system of the aromatic ring and unsaturated substituent to form the anion radical, is transferred to the C–X σ bond, which ruptures to form a carbon-centered radical and X^- .^{2,19}



Another view of this reaction is an ionic mechanism, i.e., a simple β -elimination of X^- from a negatively charged species.



The activation energies for reaction 1 involving nitrobenzylic halides (1–12 in Table I) are in the range of 11.2–15.5 kcal/mol,

(14) A small contribution to this effect may result also from changes in spin density distribution on the anion radicals in the two solvents, as expressed by the variations in their ESR parameters (Berndt, A. In "Magnetic Properties of Free Radicals" Part d1. "Organic Anion Radicals"; Fischer, H., Hellwege, K. H., Eds.; Springer-Verlag: West Berlin, 1980; Landolt-Bornstein New Series, p 430).

(15) Isied, S. S.; Kuehn, C.; Worosila, G. *J. Am. Chem. Soc.* **1984**, *106*, 1722.

(16) Huppert, D.; Kanety, H.; Kosower, E. M. *Faraday Discuss. Chem. Soc.* **1982**, *74*, 161.

(17) Butler, J.; Land, E. J.; Prütz, W. A.; Swallow, A. J. *Biochim. Biophys. Acta* **1982**, *705*, 150.

(18) Isied, S. S.; Vassilian, A. *J. Am. Chem. Soc.* **1984**, *106*, 1726, 1732.

(19) Barker, S. D.; Norris, R. K. *Aust. J. Chem.* **1983**, *36*, 81.

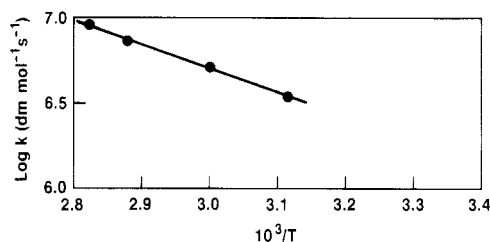


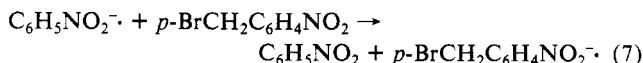
Figure 4. Arrhenius plot for a bimolecular electron-transfer reaction.

i.e., considerably lower than the values found for the $\text{S}_{\text{N}}1$ dehalogenation of similar neutral molecules.²⁰ This large difference, although it may be partly ascribed to the electrostatic effect ($\text{RX} \rightarrow \text{R}^{\cdot} + \text{X}^-$ vs. $(\text{RX})^{\cdot-} \rightarrow \text{R}^{\cdot} + \text{X}^-$), probably indicates the facilitation of the dehalogenation step by charge transfer to the halogen from the π -system of the anion radical. This charge transfer forms an unstable σ^* state which can easily revert to the more stable π^* -anion radical unless the C–X bond ruptures. Thus, even though the charge transfer is a thermodynamically uphill process, it is driven to completion by the irreversibility (at least under our conditions) of the C–X bond scission. This bond scission is the rate-determining step² of the overall process but is greatly facilitated by (and determined by the probability of) formation of the charge-transfer σ^* state. The probability of charge transfer is dependent on the spin density distribution in the π -anion radical;^{2–5} i.e., increased spin density on a ring carbon is found to facilitate dehalogenation from that position. Recent ESR study at 77 K, where the dehalogenation is prevented, has demonstrated that the anion radicals of *p*-nitrobenzyl halides exhibit a large coupling to the halogen, i.e., that there is considerable overlap between the π -system and the C–X σ bond.²¹ This overlap provides the route for the complete electron transfer to the halogen. The electron transfer can be complete only if the bond ruptures, otherwise the electron is more favorably delocalized over the π -system. Therefore, one may view the σ^* state as one of the resonance forms of the radical anion.²¹ On the other hand, it may be viewed as a distinct state if accompanied by a change in geometry,¹⁹ e.g., C–X bond twisting or stretching. This is obviously a transition state in the dehalogenation reaction.

Recent theoretical treatment of this system²² has combined molecular orbital calculations of spin densities with lattice statistical approach to estimate the relative rates of dehalogenation for *o*, *m*, and *p*-nitrobenzyl chloride anion radicals. These estimates were found to be in good agreement with the experimental results.²

Reaction Kinetics near Phase Transition Temperatures. An interesting note about the temperature dependence of the reactions is that some measurements were made at temperatures as low as -7 °C. Judging from the freezing points of ethanol–water mixtures, the freezing point of 10% *t*-BuOH in water, the solvent in these experiments, is probably -2 to -4 °C. Therefore, the present experiments were done near and below the freezing point of the solvent. The Arrhenius plots show that even at these low temperatures (at $10^3/T > 3.7$) the rate constants are not anomalous. Therefore, such possible effects as local phase transitions near the reaction site or increased viscosity or increased cage effects near the phase transition do not affect the present unimolecular dissociations. The behavior of bimolecular reactions near phase transitions would be of interest.

Activation Parameters for Bimolecular Electron Transfer. We have measured also the activation parameters for a bimolecular electron-transfer reaction that deserves a special comment:



This reaction should be very similar to the electron exchange

(20) "Tables of Chemical Kinetics. Homogeneous Reactions." *Natl. Bur. Stand. (U.S.) Circ.* **1951**, 510, and **1956**, Supplement 1.

(21) Symons, M. C. R.; Bowman, W. R. *J. Chem. Soc. Chem. Commun.* **1984**, 1445.

(22) Miller, K. E.; Kozak, J. J. *J. Phys. Chem.* **1985**, *89*, 401.

reaction between nitrobenzene and its anion radical since the reduction potentials for nitrobenzene and *p*-nitrobenzyl bromide are expected to be very similar. Reaction 7 cannot be monitored spectrophotometrically since the absorption spectra of both anion radicals are very similar. However, the product anion radical undergoes rapid dehalogenation which in this case was found to be much more rapid than reaction 7. By monitoring the dehalogenation (through the absorption of the product benzyl radical) in the presence of excess nitrobenzene and varying concentrations of *p*-nitrobenzyl bromide we can determine, therefore, the second-order rate constant for reaction 7. The value is found to be $1.9 \times 10^6 \text{ M}^{-1} \text{ s}^{-1}$, slightly higher than that determined by ESR line broadening for the self-exchange of $\text{C}_6\text{H}_5\text{NO}_2^- + \text{C}_6\text{H}_5\text{NO}_2$ ($k \sim 10^5 \text{ M}^{-1} \text{ s}^{-1}$).²³ The activation energy for reaction 7 (Figure 4) is found to be only 6.0 kcal/mol, i.e., about half the value found for the dehalogenation reaction. The activation energy for this bimolecular reaction is higher than that of the nearly diffusion-controlled²⁴ radical-radical reaction (reaction 3) only by 1.4 kcal/mol, which is sufficient to slow the reaction only by a factor

of 15. Assuming equal diffusion rates for the two reactions, reaction 7 is also slowed by a probability factor of about 0.05. Both the increased activation energy and low probability factor may be related to a geometrical reorientation required upon the reduction of ArNO_2 to form the more rigidly planar ArNO_2^- .

Acknowledgment. This work was supported by the Office of Basic Energy Sciences of the U.S. Department of Energy and by the Australian Research Grants Committee.

Registry No. (*p*- $\text{NO}_2\text{C}_6\text{H}_4\text{CH}_2\text{Cl}$)⁻, 34509-98-3; (*o*- $\text{NO}_2\text{C}_6\text{H}_4\text{CH}_2\text{Cl}$)⁻, 74261-76-0; (*p*- $\text{NO}_2\text{C}_6\text{H}_4\text{CHClCH}_3$)⁻, 83966-31-8; (*p*- $\text{NO}_2\text{C}_6\text{H}_4\text{CHClCH}_2\text{CH}_3$)⁻, 98799-24-7; (*p*- $\text{NO}_2\text{C}_6\text{H}_4\text{CCl}(\text{CH}_3)\text{C}(\text{CH}_3)_3$)⁻, 89727-62-8; (*p*- $\text{NO}_2\text{C}_6\text{H}_4\text{CH}_2\text{Br}$)⁻, 34512-14-6; (*p*- $\text{NO}_2\text{C}_6\text{H}_4\text{CHBrCH}_3$)⁻, 84024-96-4; (*p*- $\text{NO}_2\text{C}_6\text{H}_4\text{CHBrC}(\text{CH}_3)_3$)⁻, 89727-63-9; (*o*- $\text{ClC}_6\text{H}_4\text{C}(\text{O})\text{CH}_3$)⁻, 68225-75-2; (*o*- $\text{BrC}_6\text{H}_4\text{C}(\text{O})\text{CH}_3$)⁻, 77510-37-3; (*p*- $\text{BrC}_6\text{H}_4\text{C}(\text{O})\text{CH}_3$)⁻, 34473-43-3; (*p*- $\text{IC}_6\text{H}_4\text{C}(\text{O})\text{CH}_3$)⁻, 77510-38-4; (*p*- $\text{BrC}_6\text{H}_4\text{CHO}$)⁻, 77510-40-8; (*m*- $\text{ClC}_6\text{H}_4\text{CN}$)⁻, 68271-92-1; *p*- $\text{NO}_2\text{C}_6\text{H}_4\text{CH}_2$, 19019-93-3; PhNO_2^- , 12169-65-2; *p*- $\text{NO}_2\text{C}_6\text{H}_4\text{CH}_2\text{Br}$, 100-11-8; 1-(bromomethyl)-2-methyl-4-nitrobenzene radical anion, 98799-25-8; 2-(bromomethyl)-1-methyl-3-nitrobenzene radical anion, 98799-26-9; *o*-xylene, 95-47-6; 4-nitro-*o*-xylene, 99-51-4; 3-nitro-*o*-xylene, 83-41-0; 1-(bromomethyl)-2-methyl-4-nitrobenzene, 22162-14-7; 2-(bromomethyl)-1-methyl-4-nitrobenzene, 98799-27-0; 2-(bromomethyl)-1-methyl-3-nitrobenzene, 77378-54-2; 1-(bromomethyl)-2-methyl-3-nitrobenzene, 39053-40-2.

(23) Layloff, T.; Miller, T.; Adams, R. N.; Fah, H.; Horsfield, A.; Proctor, W. *Nature (London)* **1965**, *205*, 382.

(24) Hagemann, R. J.; Schwarz, H. A. *J. Phys. Chem.* **1967**, *71*, 2694. Huggenberger, C.; Fischer, H. *Helv. Chim. Acta* **1981**, *64*, 358.

Rate Constants and Mechanisms for the Reaction of OH (OD) Radicals with Acetylene, Propyne, and 2-Butyne in Air at $297 \pm 2 \text{ K}$

Shiro Hatakeyama,* Nobuaki Washida, and Hajime Akimoto

Division of Atmospheric Environment, The National Institute for Environmental Studies, Ibaraki 305, Japan
(Received: June 17, 1985)

OH (OD) radical initiated photooxidation of acetylene, propyne, and 2-butyne was studied at atmospheric pressure at $297 \pm 2 \text{ K}$. The rate constants were determined to be $(8.8 \pm 2.0) \times 10^{-13}$, $(5.71 \pm 0.18) \times 10^{-12}$, and $(3.01 \pm 0.28) \times 10^{-11} \text{ cm}^3 \text{ molecule}^{-1} \text{ s}^{-1}$ for acetylene, propyne, and 2-butyne, respectively, by the competitive reaction method using cyclohexane as a reference compound [$k_{(\text{OH} + \text{cyclohexane})} = (7.57 \pm 0.05) \times 10^{-12} \text{ cm}^3 \text{ molecule}^{-1} \text{ s}^{-1}$]. The major ultimate products are α -dicarbonyl compounds, i.e., glyoxal from acetylene, methylglyoxal from propyne, and biacetyl from 2-butyne, as well as formic acid from acetylene and propyne and acetic acid from 2-butyne. On the basis of product analyses the reaction of OH with alkynes was deduced to proceed via addition resulting in the formation of hydroxyvinyl radicals, which further react with O_2 to give carboxylic acid + RCO or α -dicarbonyl compounds.

Introduction

Although OH radical initiated oxidation of alkynes is important from the point of view of both atmospheric¹ and combustion chemistry,^{2,3} kinetic studies of this reaction under atmospheric conditions are still very limited and reaction mechanisms have not been well studied. As for the reaction mechanism, the initial step of the reaction of OH radical with acetylene has been thought to be



in earlier investigations related to combustion chemistry.²⁻⁵ Kanofsky et al.⁵ detected $\text{C}_2\text{H}_2\text{O}$ from the reaction of OH with acetylene as well as propyne under crossed molecular beam conditions using a photoionization-mass spectrometer. On the other hand, the rate constant for this reaction has recently been reported⁶⁻⁸ to be pressure dependent, e.g., varying from $\sim 3 \times$

$10^{-13} \text{ cm}^3 \text{ molecule}^{-1} \text{ s}^{-1}$ in the low-pressure region ($\leq 20 \text{ torr}$) to the high-pressure limit value of $7 \times 10^{-13} \text{ cm}^3 \text{ molecule}^{-1} \text{ s}^{-1}$ at $\geq 700 \text{ torr}$ of Ar at room temperature. From this evidence, the reaction of OH radicals with C_2H_2 at room temperature has been proposed⁶⁻⁸ to proceed via the initial addition followed by stabilization.



While the possibility of direct channels such as reaction 2 has not been excluded, Perry and Williamson⁸ suggested that such channels are minor under atmospheric conditions. A similar situation was pointed out for propyne by Atkinson and Aschmann,⁹ who reported the rate constants for the reaction of OH with a series of alkynes under atmospheric conditions.

In order to assess the atmospheric fate of alkynes emitted by fossil fuel burning¹⁰ and biomass burning,^{11,12} rate constants and

(1) Atkinson, R.; Darnall, K. R.; Lloyd, A. C.; Winer, A. M.; Pitts, J. N., Jr. *Adv. Photochem.* **1979**, *11*, 375.

(2) Jachimowsky, C. J. *Combust. Flame* **1977**, *29*, 55.

(3) Levy, J. M. *Combust. Flame* **1982**, *46*, 7.

(4) Breen, J. E.; Glass, G. P. *Int. J. Chem. Kinet.* **1970**, *3*, 145.

(5) Kanofsky, J. R.; Lucas, D.; Pruss, F.; Gutman, D. *J. Phys. Chem.* **1974**, *78*, 311.

(6) Perry, R. A.; Atkinson, R.; Pitts, J. N., Jr. *J. Chem. Phys.* **1978**, *67*, 5577.

(7) Michael, J. V.; Nava, D. F.; Borkowski, R. P.; Payne, W. A.; Stief, L. *J. Chem. Phys.* **1980**, *73*, 6108.

(8) Perry, R. A.; Williamson, D. *Chem. Phys. Lett.* **1982**, *93*, 331.

(9) Atkinson, R.; Aschmann, S. M. *Int. J. Chem. Kinet.* **1984**, *16*, 259.